FRACTURE BEHAVIOR OF ACRYLONITRILE-BUTADIENE-STYRENE RESIN

Husaini[1], and Kikuo KISHIMOTO[2]

[1] Material and Solid Mechanics Lab., Department of Mechanical Engineering, Syiah Kuala University (UNSYIAH), Darussalam – Banda Aceh 23111, Indonesia
E-mail: ftunsyiah@aceh.wasantara.net.id
[2] Department of Mechanical & Intelligent Systems Engineering, Tokyo Institute of Technology, 2-12-1, O-okayama, Meguro-ku, Tokyo 152 , Japan

Abstract

In this research, mixed mode loading testing of acrylonitrile-butadiene-styrene (ABS) resin was carried out by using a compact tension shear specimen which was attached to a special loading device. The angle between the loading axis and the crack surface was varied from 90° (Mode I) to 0° (Mode II). Two types of ABS resin were examined. The first one (ABS-1) has a butadiene rubber content of 18 wt % in the form of small particles of diameter about 200 nm. The second one (ABS-2) has the same overall butadiene rubber content but a bimodal particle distribution with diameters of 200 nm and 500 nm. Crack initiation and propagation was observed by using a video microscope. The results show that the fracture angle for both materials under mixed mode loading coincides with the values predicted by the maximum hoop stress criterion. To obtain the stress intensity factors, numerical analyses of compact-tension-shear specimen were conducted using a two dimensional finite element analysis. Fracture behavior of ABS resins under mixed mode loading was almost the same as that under mode I loading for lower value of mode II component. However, for higher mode II component, shear type fracture occurred at initial crack tip.

Keywords: *Fracture behavior, Mixed mode, ABS resin, Maximum hoop stress criterion, Crack initiation*

1. INTRODUCTION

Acrylonitrile styrene (AS) resin can be substantially toughened by the incorporation of rubber particles to give the polymer alloy. Such toughened polymers (polymer alloys) are known as ABS (acrylonitrile-butadiene-styrene) resin [1-2].

Currently, polymer alloys are widely used in many diverse industries and engineering application. To enhance the reliability of the materials, it is essential to study as complete an understanding as possible on the fracture behavior of polymer with various loading conditions. Many researchers studied fracture behavior of ABS resin in a various approach [3-5]. Huang [6] and Lu et al. [7] examined the applicability of the multispecimen J-integral method of ASTM E 813 to rubber toughened
polymers like ABS resin.

On mixed mode loading conditions Erdogan and Sih [8] studied the fracture behavior of plexiglass and proposed the maximum hoop stress criterion $\sigma_{\theta max}$ on the fracture angle θ_0 at crack initiation. The crack angle problem under mixed mode loading has also been studied on PMMA [9-10]. A large number of studies have been conducted on mixed-mode fracture of various materials [11-14]. However, little is known about fracture behavior of rubber toughened polymers under mixed mode loading. Recently, we studied crack initiation behavior of ABS resin under mode I and mixed mode loading [15]. It was found that under mode I and mixed mode loading, the fracture processes of both ABS-1 and ABS-2 are almost similarly but, the crack propagation direction under mixed mode is different from mode I case. In the ABS-2, after crack initiation, a relatively large size of membranous zone with a small hole or void appear at the crack tip. This voids become bigger and bigger until coalesce to the main crack tip. Due to such fracture process, the critical values of stress intensity factor of ABS-2 are larger for both mode I and mixed mode loading than those of ABS-1. In the previous paper, we conducted mixed mode fracture test only for one particular case of mixed mode ratio relatively low in mode II component. Therefore, the study of fracture tests for wider range of mixed mode loading from 90° (Mode I) to 0° (Mode II) is needed.

In the present paper the fracture behaviors of ABS

resins will be described for whole range of mixed mode loading. In this research, crack initiation, crack propagation and whitening zone at the crack tip are observed by using a video microscope. Moreover, the fracture surface of ABS resins is examined by scanning electron microscope (SEM). Then, fracture angle and critical values of K_I and K_{II} at crack initiation will be discussed.

2. EXPERIMENTAL PROCEDURES

2.1. Material

Both polymer alloys (ABS), and glassy polymer (AS resin) materials were chosen for this study. There are two kinds of ABS material namely ABS-1 and ABS-2, that contain 18 wt % of butadiene rubber particles consisting of single and bimodal distribution of particle diameter, respectively.

The rubber particle diameter of ABS-1 is approximately 200 nm, and there are two sizes for ABS-2 that are 200 nm and 500 nm. TEM photographs of ABS-1 and ABS-2 are shown in Fig. 1. AS resin is matrix materials of ABS and does not contain rubber particles.

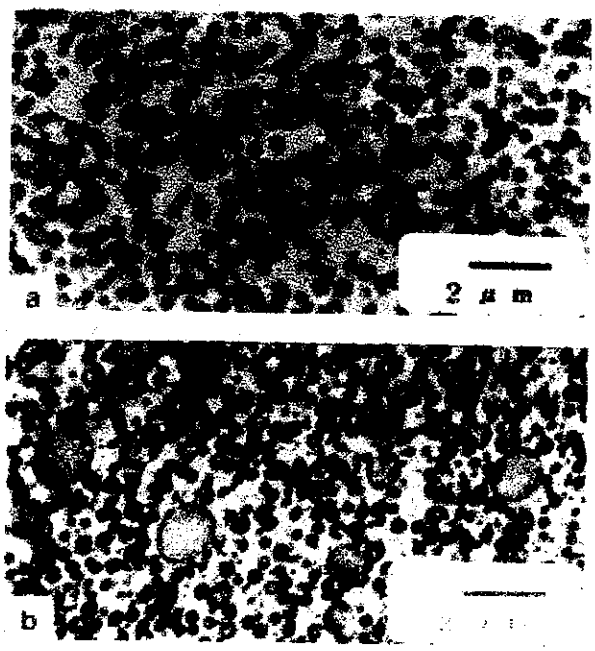

Fig. 1. TEM photograph of ABS resin with monomodal (a) and bimodal distribution of a rubber particle (b).

A compact- tension- shear specimen of dimensions 40.1 x 74 x 3.25 mm was used for fracture tests. Notch with 27.5 mm length was initially machined and initial crack was then introduced by sliding method of a razor blade, based on ASTM standards D 5045-93 [16], up to $a_o/w \sim 0.7$ (a_o = pre-crack length, w = specimen width). After a special loading device developed by Richard and Benitz [17] was attached (Fig. 2), the specimen was loaded at a constant cross head rate of 1 mm/min. Pure mode I loading was performed using No. 1 and 1' holes in the loading device shown in Fig. 2, and pure mode II loading was carried out using the No. 7 and 7' holes. The mixed or pure mode loading employing the No. n and n' holes will be referred to as the Hole No. n (n = 1, 2,....,7) loading. Crack initiation, crack growth and a whitening zone at the crack tip were observed by means of a video microscope. The initiation of the crack propagation is identified by observing the video record inversely from final state to initial state [15]. The fracture surface of ABS resins is observed by scanning electron microscopy (SEM, JSM-T200). SEM specimens were sputter-coated with a thin film of gold.

2.2. Finite Element Analysis

In order to obtain the stress intensity factors, numerical analyses of compact-tension-shear specimen were conducted using a two-dimensional finite element method with eight-noded isoparametric elements. In the FEM model, the meshes adjacent to the crack tip of the specimen were divided into fine mesh geometries. These elements were degenerating down to triangles to represent the square root stress singularity. The nodes at the crack tip were normally tied and the mid-side nodes were moved to the 1/4 point [18]. Both calculation and finite element mesh generation are conducted by employing the MARC-MENTAT II program [15, 19].

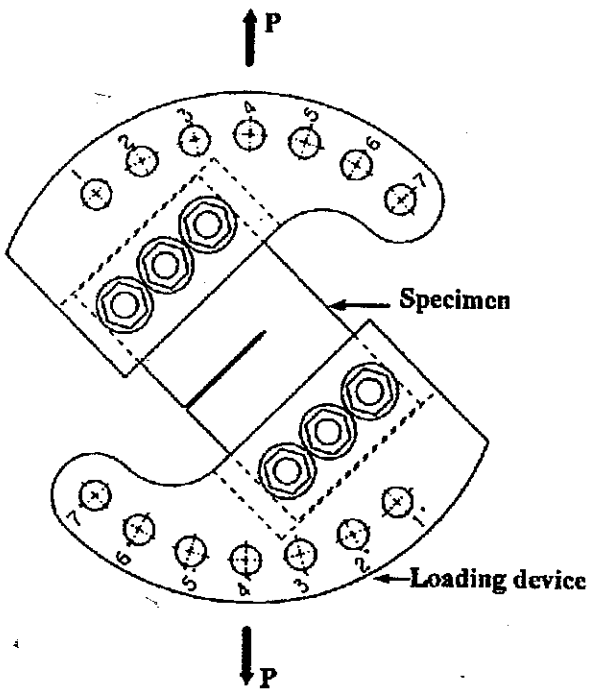

Fig. 2. Device for mixed mode loading.

3. RESULTS AND DISCUSSION

3.1 Mixed Mode Fracture Behavior

Figures 3, 4, and 5 show a relationship between applied force and cross head displacement under mixed mode loading.

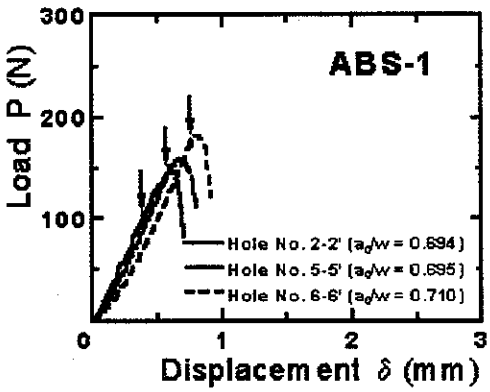

Fig. 3. Load-displacement relationships of ABS-1. Arrows indicate the crack initiation point.

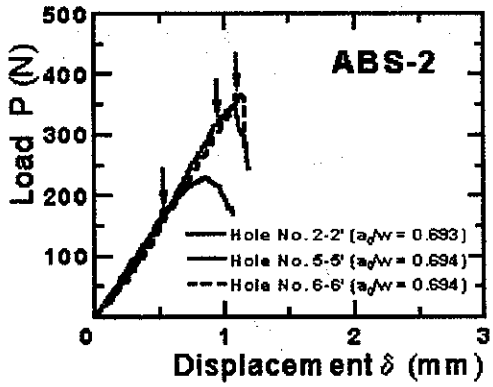

Fig. 4. Load - displacement relationships of ABS-2. Arrows indicate the crack initiation point.

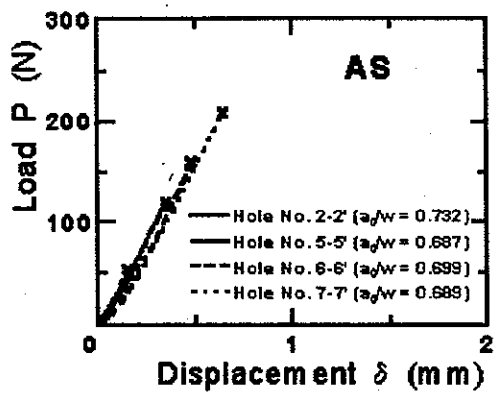

Fig. 5. Load-displacement relationships of AS resin.

The crack propagation of both ABS resins occurs in a stable manner. The arrows in these figures indicate the loads corresponding to the crack initiation identified by video record.

Figure 6 shows the crack extension in ABS-1 under mode I (Hole No. 1) and mixed mode loading (from Hole No. 2 to Hole No. 6). The appearance of the stress-whitening zone around the crack tip is due to cavitation of the rubber particle generating by hydrostatic stress [20]. A similar behavior, under mixed mode loading, is observed as in the case of mode I loading although crack propagation direction is different from mode I case. The fracture angle under mixed mode increases with an increase in mode II component as shown in the figure.

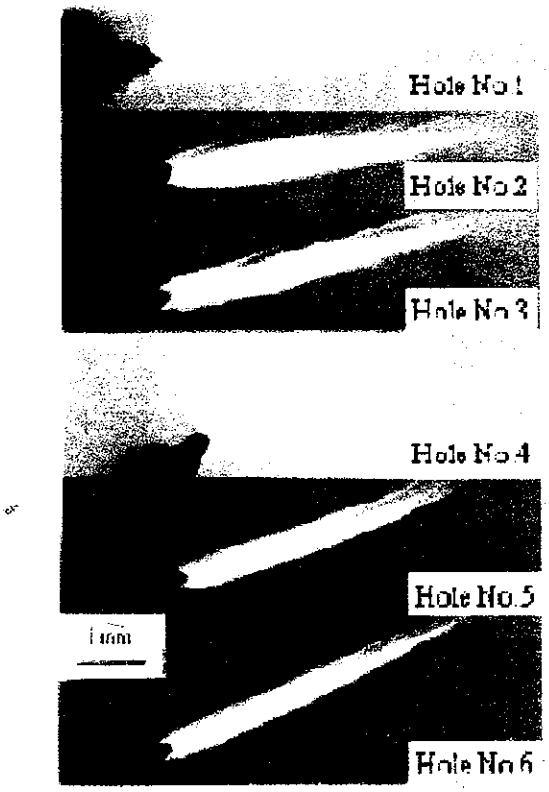

Fig. 6. Stress-whitening zone and crack extension of ABS-1. (1) K_{II}/K_I = 0. (2) K_{II}/K_I = 0.07. (3) K_{II}/K_I = 0.16. (4) K_{II}/K_I = 0.26. (5) K_{II}/K_I = 0.48 and (6) K_{II}/K_I = 0.98.

Figures 7 shows the crack extension in ABS-2 under mode I and mixed mode loading. Whitening zone expands more widely in ABS-2 than in ABS-1. Fracture process under mixed mode loading with the lower values of mode II component is almost the same as that under mode I loading as reported previously [15]. For higher mode II component (Hole No 6) there are two stages of fracture process as shown in Fig. 8. First, crack initiation occurred in shear type with the direction parallel to the initial crack tip (see frame 1). There is no whitening zone around the crack tip at this state. Then, opening

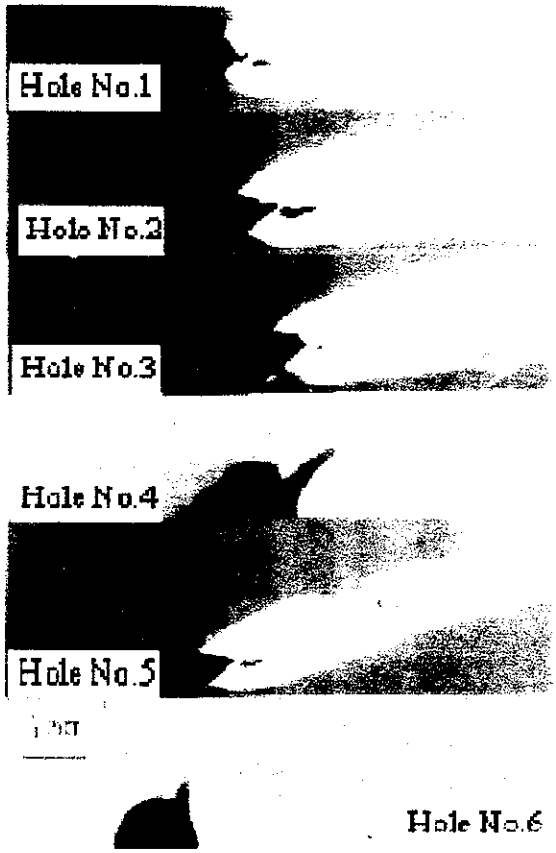

Fig. 7. Stress-whitening zone and crack extension of ABS-2. (1) K_{II}/K_I = 0. (2) K_{II}/K_I = 0.07. (3) K_{II}/K_I = 0.16. (4) K_{II}/K_I = 0.26. (5) K_{II}/K_I = 0.48 and (6) K_{II}/K_I = 1.04.

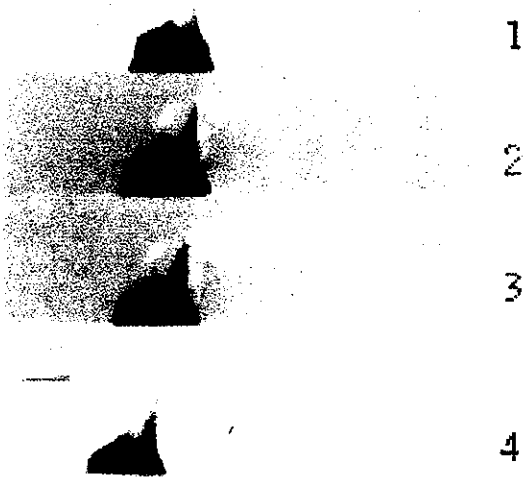

Fig. 8. Fracture process of ABS-2 under mixed mode loading (K_{II}/K_I = 1.04). (1) The direction of shear type fracture is parallel to the initial crack tip. (2)-(4) Opening type of fracture process appears on the surface of shear type fracture.

type of crack appears on the surface of shear type fracture. Next, this crack propagates inside the whitening zone, in the direction at a certain angle to the initial crack until final failure. Such fracture process was not observed clearly in the ABS-1 since the crack appears at the corner of the notch of specimen in the present experiment. This is attributable to the notch shape which has high stress concentration factor. If we could use the round notch tip shape, we would also observe the shear type fracture distinctly for ABS-1.

As shown in Fig. 9, there is no whitening zone at the crack tip of AS resin. The crack growth of AS resin occurred in unstable manner. Transition of fracture process occurring in the ABS was not observed in AS resin.

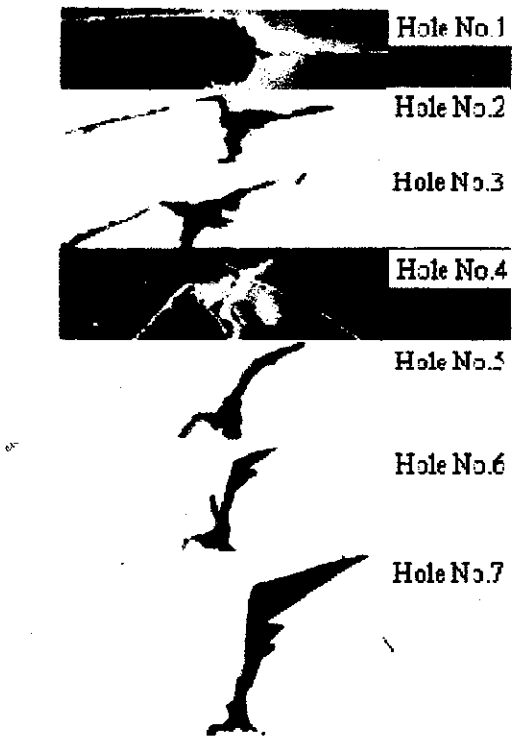

Fig. 9. Crack growth of AS resin. (1) K_{II}/K_I = 0. (2) K_{II}/K_I = 0.07. (3) K_{II}/K_I = 0.16. (4) K_{II}/K_I = 0.26. (5) K_{II}/K_I = 0.45 and (6) K_{II}/K_I = 1.05.

3.2. SEM Observation

Figure 10 shows the fracture surface of ABS-1 observed by SEM. The fracture surface under mixed mode with lower and higher in mode II component almost similar to that under mode-I loading for ABS-1. Because, after crack initiation, crack due to opening type appears soon and propagates until final failure. Therefore, the shear type fracture process could not be observed clearly under mixed mode loading with relatively lower in mode II component.

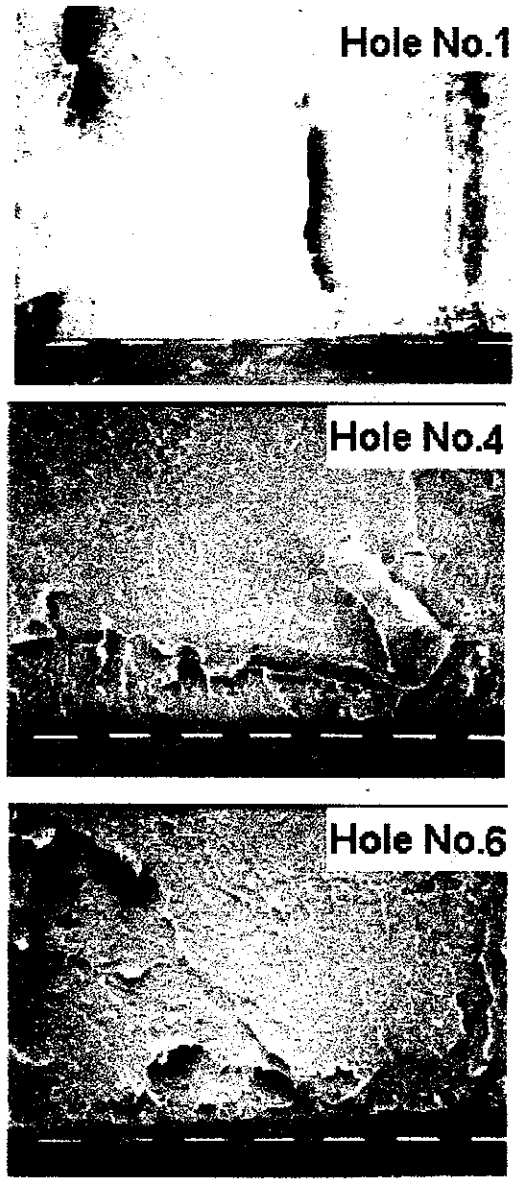

Fig. 10. SEM photograph of fracture surface around crack tip of ABS-1 (length of white line = 100 μ m).
(1) K_{II}/K_I = 0. (2) K_{II}/K_I = 0.26 and (3) K_{II}/K_I = 0.98.

Figure 11 shows SEM images of fracture surface for ABS-2. Fracture surface under loading with lower in mode II component (in this case from Hole No 1 to Hole No 5) does not indicate a significant difference.

However, the fracture surface with higher in mode II component (K_{II}/K_I = 1.04), two types of fracture surface are observed as shown in Fig. 12. The first one denoted by region (b) is the smooth region corresponding to shear type fracture. The second one denoted by region (c) is the fracture surface of opening type and has rougher fracture surface than that of the region (b).

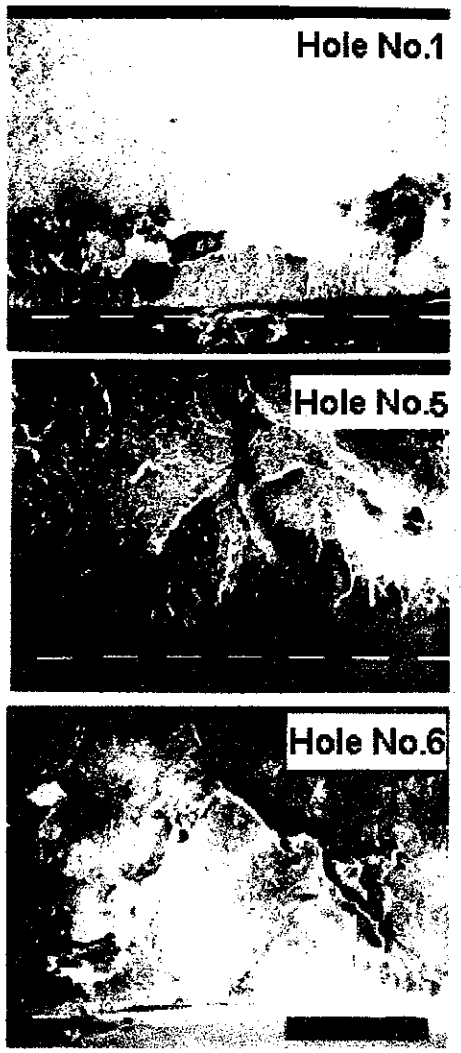

Fig. 11. SEM photograph of fracture surface around crack tip of ABS-2 (length of white line = 100 μ m).
(1) K_{II}/K_I = 0. (2) K_{II}/K_I = 0.48 and (3) K_{II}/K_I = 1.04.

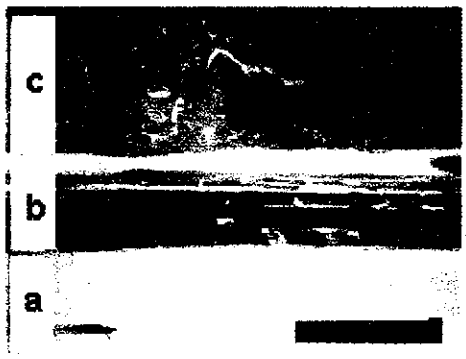

Fig. 12. SEM images of fracture surface around the crack tip of ABS-2 by high magnification (length of white line = 1000 μ m). (a) initial crack tip. (b) shear type of fracture process and (c) opening type of fracture process.

3.3. Fracture Angle and Boundary Curve

Figure 13 shows the fracture angle versus mixed mode ratio. Solid line in the figure is the prediction values by maximum hoop stress criterion. It is noted that for ABS-2 there are two values of the fracture angle under mixed mode (K_{II}/K_I = 1.04 - Hole No. 6) due to two types of fracture behavior as mentioned earlier (see Fig. 8). Shear type fracture process corresponds to the fracture angle with the value of 0^0. Except this case, the experimental and predicted values coincide with each other. This result indicates that crack propagates at the direction where the hoop stress takes maximum value.

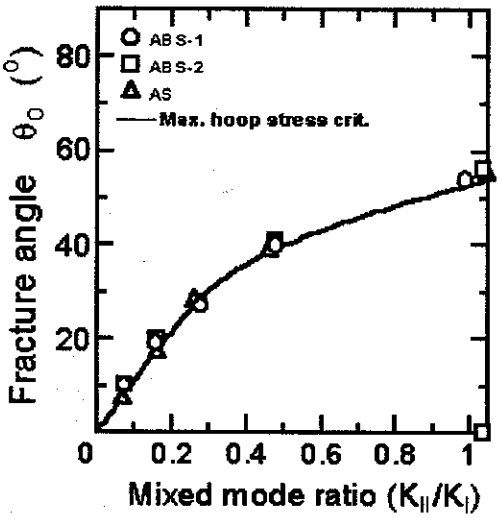

Fig. 13 Fracture angle versus mixed mode ratio (K_{II}/K_I).

Since the crack propagation occurs in a stable manner in ABS resin, the multiple specimen method is required to obtain the fracture toughness [6, 7, 21]. However, the whitening zone expansion that appears ahead of the crack tip prevents the precise measurement of crack extension Δa. Therefore, in this research a crack initiation was identified by using video recording [15]. The critical stress intensity factors K_I and K_{II} at crack initiation are plotted in Fig. 14. It is note that plotted values are for initiation of opening type of fracture. For pure mode II case, the opening type of fracture occurred at corner of initial notch, and the results are omitted here. The values of critical stress intensity factors under mode I, K_C were obtained as 0.89 MPa.m$^{1/2}$ (AS), 1.58 MPa.m$^{1/2}$ (ABS-1), and 2.42 MPa.m$^{1/2}$ (ABS-2). The values predicted by maximum hoop stress criterion, and Richard's criteria for AS, ABS-1 and ABS-2 resins are also shown in the figure. Fracture boundary curve of Richard's criterion is given by the following equations [11]:

$$\frac{K_I}{K_{IC}} + \alpha_1^2 \left(\frac{K_{II}}{K_{IC}}\right)^2 = 1 \qquad (1)$$

where,

$$\alpha_1 = \frac{K_{IC}}{K_{IIC}}. \qquad (2)$$

α_1 is considered to be a material constant and obtained by using the least square method as 1.23, 0.86, 0.36 for AS, ABS-1, and ABS-2, respectively. As shown in the figure, only the experimental results of AS resin agree well with maximum hoop stress and Richard's criterion. However, critical values of K_I and K_{II} for both ABS-1 and ABS-2 are larger than predicted values of maximum hoop stress criterion. This fact suggests that ABS resin does not follow the maximum hoop stress criterion. Both curves of Richard's criterion for ABS-1 and ABS-2 are not good agreement with the experimental data of critical values of K_I and K_{II}. Therefore, these facts suggest that the Richard's criterion can not be also applied to the ABS material.

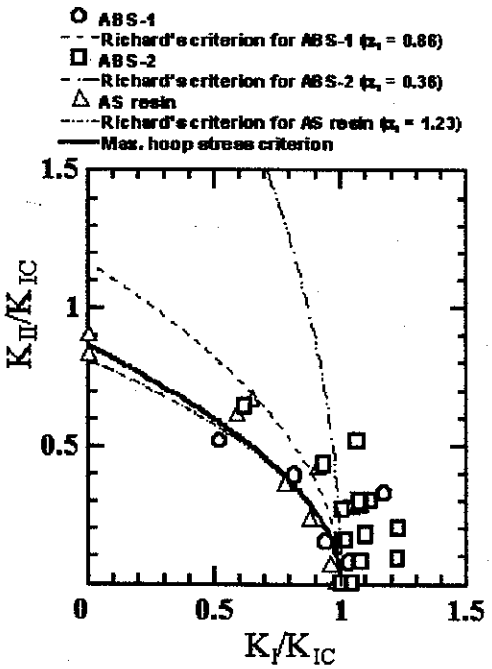

Fig. 14. K_I versus K_{II} diagram at the beginning of crack extension with fracture boundary curve.

In accordance with the results of the previous work [15], the fracture toughness K_C of ABS is larger than that of AS due to rubber particle content. In addition, fracture toughness of ABS-2 is larger than that of ABS-1. At a relatively low in mode II component value, says $K_{II}/K_{IC} <$ 0.45, the fracture resistance is higher in mixed mode loading case than pure mode I case. The tendency of fracture resistance of ABS resin deviates drastically, when $K_{II}/K_{IC} >$ 0.45. These facts imply that the transition of fracture process occurs at a certain value of mixed mode loading as mentioned above.

From SEM observation as mentioned earlier, it was found that the fracture surface is almost same but, fracture resistance increases under mixed mode loading. The increase of fracture resistance is larger for ABS-2 than for ABS-1. However, fracture resistance decreases for higher in mode II component. Especially shear type fracture appears then the fracture resistance drastically reduces as in the case of ABS-2 for mixed mode ratio $K_{II}/K_I = 1.04$.

4. CONCLUSIONS

In this study, mixed mode fracture behaviors of ABS resin have been investigated. The results obtained are summarized as follows.

1. In ABS resin, at a certain value of mixed mode loading ratio with high mode II components, crack due to shear type fracture initiates at the initial crack tip firstly. Then, another crack due to an opening type fracture occurs on the surface of the shear type fracture, and propagates until final failure.
2. The fracture angle under mixed mode loading for opening type of fracture at crack initiation coincides with the maximum hoop stress criterion for both ABS and AS resins.
3. Critical values of stress intensity factors of AS resin agree well with maximum hoop stress and Richard's criterion. Onh the other hand, both criteria are not suitable for ABS resin.
4. The critical values of stress intensity factor of ABS-2 with bimodal type of rubber particle distribution, are larger than that of ABS-1 with monomodal type distribution of rubber particle, for both mode I and mixed mode loading.
5. Fracture resistance of both ABS-1 and ABS-2 resins increases under mixed mode loading with the relatively lower in mode II component. However, the fracture resistance reduces at a certain mode II component under mixed mode loading due to shear type of fracture.

5. ACKNOWLEDGMENTS

The authors express their thanks to Japan Synthetic Rubber Co. Ltd. for contributing specimens.

6. REFERENCES

1. A.J., Kinloch, and R.J., Young, *Fracture behavior of Polymer*, Applied science publishers, London, (1983).
2. C. K., Riew, and A. J., Kinloch, ed., *Toughened Plastics II: Novel Approaches in Science and Engineering, Advances in Chemestry Series 252*, Washington, DC. (1996).
3. A. M., Donald, and E. J., Kramer, Plastic Deformation Mechanism in poly(acrylonitrile-butadiene styrene) [ABS], *J. Mater. Sci.*, **17**, 1765-1772, (1982).
4. B. Y., Ni, T. Y., Zhang, and J. C. M., Li, A New Approach to Fracture Toughness Analysis and Its Application to ABS polymers, *J. Mater. Res.*, **6, 6**, 1369-1373, (1991).
5. Wu, J. S., Shen, S. C., and Chang, F., C., Effect of Rubber Content in Acrylonotrile-Butadiene-Styrene and Additional Rubber on The Polymer Blends of Polycarbonate and Acrylonitrile-Butadiene-Styrene, *Polymer Journal*, **26, 1**, 33-42, (1994).
6. D.D., Huang, *In Toughened Plastics I: Science and Engineering, Riew, C. K., and Kinloch, A. J., Ed.; Advances in Chemestry Series 233*; American Chemical Society, Washington, DC, 1993.
7. M. L., Lu, C. B., Lee, and F. C., Chang, Fracture Toughness of polycarbonate/ acrylonitrile-butadiene-styrene blend by the ASTM E813 and hysteresis energy J integral methods: effect of specimen thickness and side groove, *Poly. Eng. and Science*, **35, 18**, 1433-1439, (1995).
8. F. Erdogan, and G. C. Sih, On the Crack Extension in Plates Under Plane Loading and Transverse Shear, *J. Basic Eng.*, **85**, 519-527, (1963).
9. J. G. Williams, and P. D. Ewing, Fracture Under Complex Stress - The Angle crack Problem, *Int. J. Fracture Mech.*, **8, 4**, 441-446, (1972).
10. I. Finnie, and A. Saith, A Note on The Angled Crack Problem and The Directional Stability of Cracks, *Int. J. Fract.*, **9**, 484-486, (1973).
11. H. A. Richard, Crack Problems Under Complex Loading, *Int. Conf. on Role of Fracture Mechanics in Modern Technology, Sih, G. C., Nisitani, H., and Ishihara, T., Ed.*, Fukuoka, Japan, 577-588, (1986).
12. A. Otsuka, K. Tohgo, and Y. Okamoto, Relationship Between Ductile Crack Initiation and Void Volume Fraction, *Nuc. Eng. Design*, **105**, 121-129, (1987).
13. S. Aoki, K. Kishimoto, T. Yoshida, M. Sakata, and H. A. Richard, Elastic-Plastic Fracture Behavior of An Aluminum Alloy under Mixed Mode Loading, *J. Mech. Phys. Solids*, **38, 2**, 195-213, (1990).
14. T. Kuriyama, and I. Narisawa, Fracture Behavior of Ductile Polymer Under Mixed Mode Loading, *Proc. Annual Technical Conference-ANTEC*. Soc. of Plastics Engineer, USA, Brookfield, .3235-3239, (1994).

15. Husaini, M. Notomi, K. Kishimoto, and T. Shibuya, Crack Initiation Behavior of ABS resin Under Mode I and Mixed Mode Loading, *Mater. Sci. Res. Int.*, **3**, 3, 158-165, (1997).
16. Standard Test Methods for Plane-Strain Fracture Toughness and Strain Energy Release Rate of Plastic Materials, *ASTM D 5045-93*, (1994).
17. A. Richard, and K. Benitz, A Loading Device For The Creation of Mixed Mode in Fracture Mechanics, *Int. J. Frac.*, **22**, R55-R58, (1983).
18. T. L. Anderson, *Fracture Mechanics Fundamentals and Application*, CRC Press, Inc., Boston, (1991).
19. MARC User's manual, *MARC Analysis Research Corporation*, California 94306 USA, (1994).
20. A. Collyer, *Rubber Toughened Engineering Plastics*, Chapman & Hall, (1994).
21. Notomi, K. Kishimoto, and T. Koizumi, Fracture Behaviours of Polycarbonate and Cellulose-Acetate Exposed Under High Humidity, *Proc. 9th Int. Conf. on Deformt., Yield and Fracture of Polymers*, Cambridge, UK., p43/1-p43/4, (1994).